International Journal of Research and Development in Engineering Science
ISSN: 2582 - 4201(Online) , http://www.ijrdes.com/
Regular Issue, Vol. 6, Issue. 3 (May – June), 2024 , Pages: 1-10
Received: 20 April 2024 ; *Accepted:* 1 May 2024 ; *Published:* 10 May 2024
https://doi.org/10.63328/IJRDES-V6RI3P1
Original Paper : Applied Research - Experimental Research Paper

CT Liver Tumor Segmentation using a Hybrid Deep Convolutional Neural Network RA-UNet

P. Gangadhara Reddy [1*], Avvaru Subramanyam [2], T. Ramashri [3]

[1*] Department of ASCE, Aditya College of Engineering, Madanapalle, Andhra Pradesh, India; gangadharareddy.p@gmail.com
[2] Department of ASCE, Vignan's Foundation for Science, Technology & Research, Guntur, India
[3] Department of ECE, Sri Venkateswara University College of Engineering, S.V. University, Tirupati, A.P , India

* *Corresponding Author:* gangadharareddy.p@gmail.com

Abstract: Convolutional Neural Networks (CNNs) have currently acquired focus from researchers to address computer vision and medical image processing problems. Popular though they may be, most methods can only handle 2D pictures, but in medical liver tumor segmentation 3D volumes are normally analyzed in clinical data. Here, we offer a technique for segmenting 3D images using a fully convolutional neural network that has been trained on volumetric data. Our CNN is taught to predict segmentation for the entire volume simultaneously after being trained from scratch on prostate Magnetic Resonance Imaging (MRI) data. Liver cancer is second among male cancers in terms of mortality and sixth among female cancers in terms of mortality. Diagnosing, treating and assessing the efficacy of liver cancer all rely on accurate segmentation of hepatic lesions. As a standardized benchmark, LiTS (Liver Tumor Segmentation Challenge) allows researchers to evaluate and compare several automated liver lesion segmentation approaches. Computed tomography (CT) allows for early diagnosis, which is key to a high recovery rate. However, manually reviewing CT slices for thousands or millions of patients is difficult, tiring, costly, time-consuming, and prone to mistakes. Thus, we need a trustworthy, easy, and precise approach to automating this procedure. This work contains convolutional neural networks (CNNs) to solve all those problems; specifically, a trained RA-UNet(or) Res U-Net model using the 3D-IRCADb01 dataset, which includes CT slices from patients and masks for liver, tumors, and other organs. RA-UNet model combines the U-Net and ResNet models, instead of using convolutional blocks, it employs Residual blocks A second CNN was trained to segment the tumours based on the output of the first CNN after a first Cascaded Convolutional Neural Network (CNN) was used to segment the liver and extract the ROI. The dice coefficient was 95%, while the True Value Accuracy was 99%.

Keywords: Liver, Computed Tomography, Segmentation, Tumor Extraction, U-Net, Residual Learning.

1. Introduction

The most vital organ is the liver because of its role in detoxifying. Oncologists and radiologists use CT and MRI scans to examine livers for irregularities in structure and texture. Both primary and secondary hepatic tumors may be detected and tracked with the use of these abnormalities [1]. Primary abdominal tumours, including those from the breast, colon, and pancreas, frequently spread to the liver. Primary tumor staging always includes an examination of the liver and its abnormalities. The RECIST methodology, which mandates that the greatest target lesion's diameter be recorded, has become the gold standard for clinical use in tumor staging of liver cancer [2]. The second most common cause of cancer-related death worldwide and the sixth most common disease overall is primary liver cancer. Radiologists and oncologists rely heavily on CT scans to assess liver lesions, determine their severity, and stage the disease. Furthermore, malignant liver tissue segmentation is essential for the diagnosis, therapy, planning, and monitoring of cancer. However, diagnostic images are costly, time-consuming, seldom repeatable, and exhibit operator-dependent outcomes when segmenting. Hepatic tumors, often liver tumors, pose a significant risk to human health. Liver cancer, or a malignant tumor, is one of the most common types of cancer (6% incidence globally) and a significant cause of cancer-related mortality (9%). [3]. Sometimes benign (not malignant) tumors might get big enough to be problematic for a patient's health. For diagnosis, computed tomography (CT) is used in the case of liver tumors. Before deciding on a surgical procedure, removing the liver and tumors from the CT scan is

ISSN: 2582 - 4201(Online) , http://www.ijrdes.com/ , IJRDES, Vol. 6, Issue 3 , 2024 , https://doi.org/10.63328/IJRDES-V6RI3P1

essential. The specific locations of the liver and tumor in the human body may be determined by careful medical imaging segmentation. Specialists' assessments of patients' needs will pave the way for the delivery of tailored therapy [4]. However, it is difficult to divide liver and tumor from CT scans owing to their heterogeneous and diffuse forms. The liver/tumor segmentation job has been the subject of several attempts. CT images of the liver and tumors segmentation as shown in figure 1.

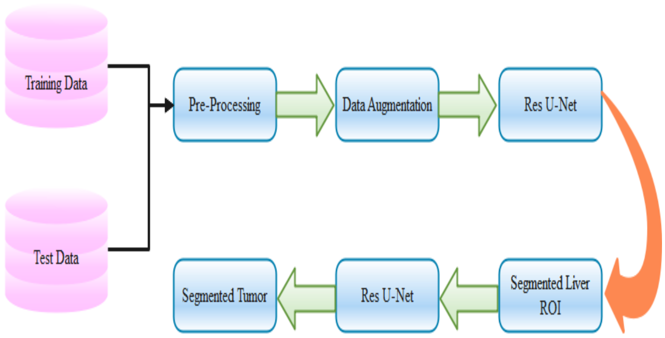

Figure.1 Overview of the proposed workflow

The methods for extracting the liver and tumours may be broken down into three broad classes: manual segmentation, semi-automated segmentation, and automated segmentation. In contrast to automated methods, manual segmentation is labor-intensive and prone to error. Human distinguishable traits play a crucial role, and specialists with advanced technological knowledge are needed to carry out these jobs. Because of these drawbacks, its use in actual settings is not feasible [5]. Because of the need for human interaction at the outset, semi-automated segmentation is prone to prejudice and errors. There is a pressing need to provide an automated and accurate approach to segment tumors from CT scans to speed up and simplify diagnosis, treatment planning, and monitoring and ultimately aid surgeons in removing malignancies.

However, automating segmentation is challenging because of the high degree of spatial and structural variability, the lack of contrast between liver and tumor regions, the presence of noise and partial volume effects, the complexity of 3D-spatial tumor features, and the similarity between tumors and neighboring organs. Many segmentation of volumetric images has recently been performed using convolutional neural networks (CNN) [6]. Both 2D and 3D convolutional neural network models have been constructed. However, in most cases, 3D networks are less productive and adaptable than their 2D counterparts. Semantic segmentation, for instance, has been suggested for 2D and 3D fully convolutional networks (FCNs) [7]. However, the depth of the 3D FCNs is restricted compared to that of the 2D FCNs because of the high computational cost and GPU memory consumption, making the extension of the 2D networks to the 3D networks difficult. We propose RA-UNet, a hybrid residual attention-aware liver and tumor extraction neural network, to address these problems and is motivated by the attention mechanism and residual networks.RA-UNet is created to efficiently extract 3D volumetric contextual features of the liver and tumor from CT images in an end-to-end manner [8]. The suggested network optimizes and improves the performance of extremely deep networks by combining a U-Net design with a residual network learning technique. Our research is the first to take advantage of the residual network mechanism for segmenting medical images. To begin, we solve the gradient vanishing issue by stacking leftover blocks in our design, making it deeper. As a second point, the attention mechanism may be able to zero in on certain picture regions. Adaptive attention-aware features may be implemented using a variety of attention kinds made feasible by stacking attention modules. Finally, the 2D/3D U-Net is the foundational architecture that employs to gather multi-scale attention information and combine low-level characteristics with high-level ones. In addition, it's important to note that our liver/tumor segmentation strategy employs a fully 3D network to do the segmentation from beginning to finish. This model doesn't need pre-training or standard post-processing methods like other models. By applying the method to various datasets, show that it is generalizable. On the MICCAI 2017 Liver Tumor Segmentation (LiTS) dataset and the 3DIRCADb dataset [9], this design not only extracts correct liver and tumor areas but achieves competitive performances compared to current state-of-the-art approaches. In addition, RA-UNet may be used for additional medical picture segmentation problems by extending it to brain tumor segmentation.

2. Background and Earlier Efforts

The liver and liver tumor segmentation process involves locating the voxels in medical imaging that best characterizes the liver and tumor regions. The last decade has seen a fourfold increase in liver and liver tumor segmentation research. Most existing semi-automatic liver, and tumor segmentation approaches rely on standard computer vision and machine learning techniques. When using machine learning-based techniques, multiclass categorization of liver and tumor voxel/pixel is often employed. The next part summarizes previously reported approaches to semi-automated liver and liver tumor segmentation.

2.1. Review of Liver Segmentation Algorithms

The literature on liver segmentation methods can be divided into four groups: those that rely on spatial and geometrical prior knowledge, those that use local image

ISSN: 2582 - 4201(Online) , http://www.ijrdes.com/ , IJRDES, Vol. 6, Issue 3 , 2024 , https://doi.org/10.63328/IJRDES-V6RI3P1

features with a unique context, and those that use local image features with voxel-wise classification, and those that employ neural networks. In addition, the segmentation strategies mentioned earlier may be used to create semi-automated solutions.

Spatial and geometrical previous knowledge-based techniques

Since the early 2000s, automatic liver segmentation has used Statistical Shape Models (SSMs). However, due to deformation constraints, SSMs cannot capture the very variable liver shapes. Several SSMs methods take an extra step toward creating a more precise segmentation contour to get this issue. As a result, SSMs followed by a deformable model carrying out free form deformation have shown to be a valuable technique for liver segmentation.

In addition, numerous variants and improvements of SSM have been proposed to automatically solve liver segmentation tasks, including 3D-SSM based on an intensity profiled appearance model, incorporation of non-rigid template matching, initialization of SSMs using an evolutionary algorithm, hierarchical SSMs, and deformable SSM [10].

Techniques based on spatial context and local image features

Gray level techniques use statistical modeling to approximate the liver's intensity distribution. Lim et al. suggest different approaches to segmenting the liver using morphological filters, intensity distributions, and pattern features. Graph Cut (GC) techniques separate the picture into the front and liver. Images are represented by a set of vertices, one for each pixel or voxel.

Adaptive thresholding and super voxel-based graph cuts are described automatically in various ways [12]. In addition, random walk algorithms with autonomous liver tumor recognition may be used for seed generation, fuzzy c-means based clustering, and artificial bee colony clustering with morphological operations to improve segmentation [13].

Local image characteristics using voxel-wise classification

Rarely some classification methods that only look at liver segmentation without tumors. Current methods include a combination of AdaBoost classifier for site identification or liver boundary detection and free-form deformation for segmentation elaboration. AdaBoost is used in conjunction with random walk algorithms in other feature-based categorization methods [14].

Neural network and deep learning-based techniques

Histogram characteristics were employed in the first proposed neural network for liver segmentation in 1994. Pre- and post-processing played a significant role in the method, with the former used to eliminate extraneous areas up front and the latter used to guarantee clean borders via morphological operations and b-spline smoothing. In contrast to traditional neural networks, modern convolutional Neural Networks are data-driven and allow for end-to-end optimization without requiring feature engineering. Convolutional neural networks are often used for semantic segmentation tasks in medical imaging that don't require well-made features [15].

Since its introduction by Ronneberger et al., the U-Net architecture has become a popular deep convolutional neural network (DCNN) for biomedical image segmentation. Combining an equal number of upsampling and downsampling layers with skip connections between its opposing convolution and deconvolution layers is the architectural innovation in U-net compared to conventional semantic segmentation networks [16]. Other methods, including U-NET, which also employed 2D CNN but without cross-connections, overcame the difficulty of poor contrast between the liver and neighboring organs and showed promising results on SLIVER07.

These algorithms employ a 3D convolutional neural network (CNN) as the foundation, feeding the probability maps it generates into further post-processing steps. Both simultaneous liver detection and probabilistic segmentation using 3D CNN, as well as subsequent accuracy refinement of the segmentation using graph cut, 3D CNN in combination with random fields, and 3D CNN following a surface evolution algorithm [17], have shown promising results on SLIVER07. Additionally, a subject-specific probability map of the liver has been suggested to be learned using a 3D convolutional neural network. After that, a segmentation model is built that is globally optimized for surface evolution, taking into account both global and local appearance information.

Methods that are only partly automated

Automated segmentation methods need a large dataset to model the varying liver structures. In the case of abnormal livers, semi-automatic methods were generally considered more reliable. However, the segmentation outcomes of semi-automatic approaches vary depending on the operator's expertise. There are a variety of semi-automated approaches, each requiring a unique level of human intervention. Region growth is a widespread technique, although it often requires time-consuming and expensive pre- and post-processing in the form of manually

ISSN: 2582 - 4201(Online) , http://www.ijrdes.com/ , IJRDES, Vol. 6, Issue 3 , 2024 , https://doi.org/10.63328/IJRDES-V6RI3P1

initializing seed regions and refining segmentation. In contrast, state-of-the-art region-expanding approaches achieve competitive outcomes in 2D liver segmentation and 3D liver segmentation. As a result of its semi-automatic capability to change segmentation findings interactively, Graph Cut (GC) segmentation approaches are well suited for clinical applications. Refining the liver segmentation using GC requires more expensive user input [18]. In addition, slice-based segmentation employing distance transformations of manually segmented upper and lower axial slices and 2D to 3D interpolation approaches based on shape models to rebuild the full 3D surface based on chosen 2D contours are suggested. In addition to manual seeding and k-means clustering, other 3D segmentation methods include active contour-based segmentation using surface information provided by a level set method and a single manual seed inside the liver and a contouring algorithm for advanced segmentation based on a manually selected single slice [19].

2.2. Liver Tumor Segmentation Algorithms

Tumors in the kidney seem different in size, color, and texture than those in the liver. Compared to segmenting a single area of interest, liver tumors commonly arise in clusters and lack distinct borders. It's common for contrast agents to increase image noise. As a result, identifying and separating tumors in the liver is viewed as the more difficult of the two tasks. Thresholding methods, Spatial regularisation methods, Local image features with supervised classification and unsupervised clustering methods, Deep Learning methods, and so on are all published approaches to liver tumor segmentation. In addition, the strategies mentioned above may be used to create semi-automated solutions.

Threshold techniques

Thresholding is a simple but effective approach to automatically differentiating tumor from liver and background, as shown for the first time by Gotra, A et al. 2017 [20]. Thresholding works on the premise that grey levels of tumor areas vary from pixels corresponding to regions outside the tumor. Since then, thresholding-based approaches have been developed to optimize tumor segmentation outcomes via the use of histogram analysis, maximizing variance across classes, and iterative adjustment of the threshold value using an iso data algorithm.

Regularization strategies in spatial

Spatial control methods require (initial) data about the image or morphologies, such as tumor size, shape, surface area, and location. This information is then used to impose constraints in the form of regularisation or penalty. When dealing with heterogeneous lesions, it is possible to use a combination of model-based morphological processing and adaptive thresholding techniques. Tumor segmentation based on active contours uses probabilistic models or histogram analysis to generate segmentation maps automatically based on shape and surface information. Numerical calculations of tumor forms are now possible without parametrization using level set approaches. The segmentation of liver tumors is performed using a level set method in conjunction with supervised pixel classification in 2D and 3D. Furthermore, the probability vectors from the starting 2D CNN are used to parametrize one suggested level set method.

Supervised classification and unsupervised clustering techniques for local image features

Machine learning-based approaches are well-established in automated liver tumor segmentation tasks due to the liver tumor heterogeneity. The methods for grouping similar items include k-means clustering and fuzzy c-means clustering with segmentation refinement using deformable models. A fuzzy classification-based level set approach, Support Vector Machines (SVM) with a texture-based deformable surface model for segmentation refinement, AdaBoost trained on texture features and image intensity profiles, logistic regression and Random Forests (RF) recursively classifying and decomposing supervoxels [21] are all examples of supervised classification techniques.

Techniques of Deep Learning

The use of deep learning techniques for liver tumor segmentation has been limited before LiTS. Christ, P. F et al. [22] proposed a dense 3D conditional random field for segmentation refinement following cascading 3D CNNs (U-Net) for liver and tumor segmentation. At the same time introduced an 11-layer 3D CNN and graph cut for segmentation refinement.

Semi-automated methods

Tumors of the liver can take on a wide variety of sizes, textures, colors, and numbers of cells. As a result, many different semi-automatic strategies have been proposed. Some of the methods used in the published work include: graph cut followed by watershed for refined segmentation, adaptive multi-thresholding based on cross-entropy with level set techniques for segmentation refinement, bayesian classification with active contours refinement relying on manually selected seeds[30], an Extreme Learning Machine (ELM) ensemble where each member is trained on a random feature subspace of manually selected 3D samples, and support vector machines for an iterative 2D slice

ISSN: 2582 - 4201(Online) , http://www.ijrdes.com/ , IJRDES, Vol. 6, Issue 3 , 2024 , https://doi.org/10.63328/IJRDES-V6RI3P1

3. Methodology

Overview of proposed architecture

The segmentation architecture in figure 2. The suggested design has three primary phases that sequentially harvest liver and tumor. A 2D Residual Attention-aware U-Net (RA-UNet) is used based on a residual attention mechanism and U-Net connections to identify a rough liver boundary box [24]. The name RA-UNet-I to cut down on computation time. A 3D RA-UNet (RA-UNet-II) was trained to get an accurate liver VOI. At last, the outlined liver VOI was sent to a second RA-UNet-II to isolate the tumor zone. The developed network can process large amounts of data under various challenging situations, producing good outcomes across many liver/tumor datasets.

Materials and data sets

As part of our research, we put this framework through its paces using the open-source Liver Tumor Segmentation Challenge (LiTS) dataset. There are 200 CT scans, 130 of which are training data and 70 as test data. Both sets of scans have an in-plane resolution of 512x512. However, the number of axial slices varies. The ground truth of the training data is supplied by several clinical locations all over the globe, but the same cannot be said for the test data. Our model's generalizability and scalability are evaluated using an external test dataset called 3DIRCADb. Twenty cancers from European hospitals were manually segmented using improved CT images. Each scan has a unique number of 512x512 in-plane resolution axial slices.

Datasets on livers and liver tumors public datasets

The liver is an organ that has received very little attention in the field of tumor segmentation in CT imaging. The primary reason is that there are not enough publicly available datasets that are both large and meticulously annotated [25]. Available datasets provide either a small number of images or no ground truth segmentation is shown in table 1.

Table.1 Ground truth segmentation for liver images

Dataset	Institution	Liver	Tumor	Ground Truth	#Volumes	Modality
3Dircadb-01	IRCAD	3	3	3	20	CT
3Dircadb-02	IRCAD	3	3	3	2	CT
Sliver'07	MICCAI	3	7	3	30	CT
TCGA-LIHC	TCIA	3	3	7	1688	CT, MR, PT
MIDAS	IMAR	3	3	7	4	CT

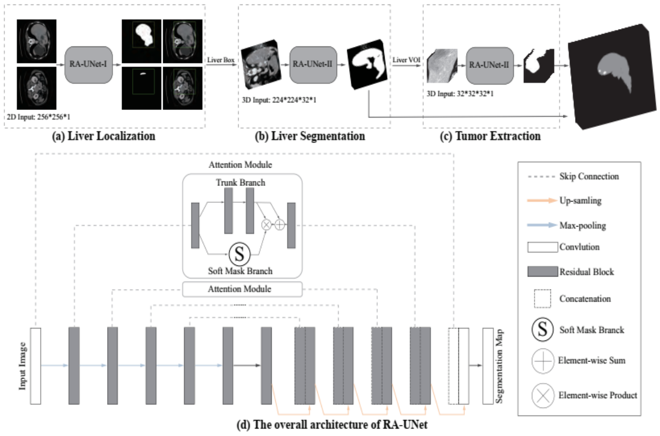

Figure 2: High-level perspective of the proposed segmentation process for liver and tumor detection.

(a). Coarse localization of a liver area inside a border box is performed using a simplified version of 2D RA-UNet (RA-UNet-I).
(b). Liver VOIs inside the liver border box may benefit from the hierarchical extraction of attention-aware features using the 3D RA-UNet (RA-UNet-II).
(c). Precise tumor extraction inside hepatic VOIs is the responsibility of RA-UNet-II.
(d). (d)In particular, we will focus on RA- UNet's overarching structure.

Preprocessing of Data

Hounsfield units (HU) are a CT-based relative density measurement for a medical image's volume. Typically, HU values are shown in a range from -1000 to +1000. Tumors in the liver can be complicated by the presence of bones, air, or irrelevant tissues in the vicinity. Since these sounds were undesirable, a first segmentation was performed to remove them, leaving the liver area ready for further analysis. Data preparation through global windowing was chosen due to its practicality and efficiency.

Table 2. Range of HU values in various tissues

HU values for body organs	
Bone	1000
Liver	40 to 60
White Matter	46
Grey Matter	43
Blood	40
Muscle	10 to 40
Kidney	30
Cerebrospinal	15
Water	0
Fat	-50 to -100
Air	-1000

Table 2 displays the vast range of HU values in various tissues by tabulating their usual radio densities. Three-dimensional coronal, sagittal, and axial plane views of the

ISSN: 2582 - 4201(Online) , http://www.ijrdes.com/ , IJRDES, Vol. 6, Issue 3 , 2024 , https://doi.org/10.63328/IJRDES-V6RI3P1

raw volumes in LiTS and 3DIRCADb used in this work. The volumes before processing, with unnecessary organs eliminated, are shown in the second row. The majority of the background noise has been eliminated.

The Proposed Network Architecture

Figure 1 depicts the general layout of the network. It has two distinct sides: one that contracts (on the left) and one that expands (right). The shortening route is laid out in the conventional fashion of a convolutional neural network. Two 3x3 convolutions (unpadded convolutions) are applied, followed by a rectified linear unit (ReLU) and a down sampling 2x2 max pooling operation with stride 2. As we go through the down sampling process, we double the number of feature channels. Each iteration of the expansion path begins with a 2x2 convolution (up-convolution) that halves the number of feature channels, then moves on to a concatenation with the cropped feature map from the contraction path and concludes with two 3x3 convolutions, each of which is followed by a ReLU. Due to the inevitable loss of boundary pixels in every convolution, cropping is required. Each 64-component feature vector is then mapped to the target number of classes using a 1x1 convolution in the final layer. The network consists of a total of 23 convolutional layers. It is crucial to choose the input tile size so that all 2x2 max-pooling operations are applied to a layer with an even x and y size, as shown in Figure 2, to allow for seamless tiling of the output segmentation map.

The design of the RA-UNet

In [25], the authors integrated the share-net with attention mechanisms to improve semantic picture segmentation, making it the first work. The attention mechanism has been slowly used in medical picture segmentation in recent years. For liver tumor segmentation, we propose the RA-UNet, a "very deep" architecture influenced by both residual attention learning and U-Net [26]. A network may contain hundreds of layers thanks to the residual block, and the attention mechanism can learn to zero down on essential areas for discerning objects of interest. The network architecture is shown in figure 3 and it consists of a contracting path and an expansive path and it consists of a total of 23 convolution layers.

ii) U-Net as the primary frameworks

This RA-UNet, looks like a traditional U-Net, is bidirectionally symmetrical, with an encoder and a decoder on opposite ends. The encoder spreads the contextual information over the rich skip connections to extract more complicated hierarchical features. The characteristics sent to the decoder might range in complexity. Thus it reconstructs them from course to fine. To blend distinct hierarchical characteristics from the encoder to the decoder, the U-Net offers long-range connections between the encoder and the matching decoder, significantly improving the network's accuracy and scalability.

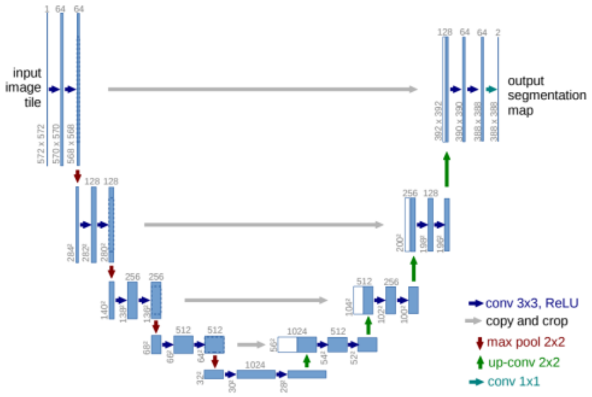

Figure.3 Architecture of the Conventional U-Net.

The mechanism of residual learning:

The significance of the network depth cannot be overstated. However, gradient vanishing is a typical issue when training a sufficiently deep neural network, leading to poor outcomes. To get over this issues to overcome using a deep residual learning framework to study the residual of the identity map. Our research stacks residual blocks between layers two and three, allowing a deep neural network to "go deeper". Stacked residual blocks can address the gradient vanishing issue in neural networks at a structural level through the use of identity mappings as skip connections and after-addition activation. The model's performance is enhanced as a direct result of the residual units' ability to relay features from early to late convolution. This is what we mean by the term "residual block."

$$RB_{pn}(x_{in}) = x_{in} + f_{pn}(x_{in}) \quad (1)$$

Here x_{in} First input of Residual block, RB is the Residual block output,nɛ{1,2,….N}index channels,n indicates all spatial positions,N represents channels are there in total, and f is the residual mapping that has to be learned. The residual block comprises a batch normalization (BN) layer, an activation (ReLU) layer, and a convolutional layer. As the network "deepens," the convolutional identity mapping connection is used to maintain accuracy. Figure 5 depicts the residual unit in all its graphical richness.

Mechanism for retaining focus on something is the attention residual

The performance will suffer if just naïve stacking is employed for the attention modules. Wang et al. [24]

ISSN: 2582 - 4201(Online) , http://www.ijrdes.com/ , IJRDES, Vol. 6, Issue 3 , 2024 , https://doi.org/10.63328/IJRDES-V6RI3P1

suggest a method for addressing this problem using attention residual learning. To process the original features and build the identity mapping, the attention residual mechanism splits the attention module into a trunk branch and a soft mask branch. Under attention residual learning, the attention module's output OA can be expressed as

$$OA_{pn}(x_{in}) = (1 + S_{pn}(x_{in}))F_{pn}(x_{in}) \qquad (2)$$

where the range of S(x) is [0,1]. Feature maps F can be approximated by OA(x) if S(x) is close to 0. The most crucial part of the attention residual mechanism is played by the soft mask branch S(x), which picks up on similar features and dampens the noise in the trunk branch. The soft mask subtree encoder-decoder structure has been extensively used in medical picture segmentation [27]. The residual attention mechanism was developed to improve feature quality while decreasing noise in the trunk/branch structure. The soft mask branch encoder performs an element-wise sum after an up-sampling operation and a residual block. In contrast, the equivalent decoder uses a max-pooling operation, a residual block, and a long-range residual block. Two convolutional layers and a sigmoid layer are added to the output of the soft mask network after the encoder and decoder portions. The residual attention module is shown in graphical detail in Fig. 4. When it comes to liver tumors, the residual attention mechanism may remember the initial feature data through the trunk branch and focus on the relevant characteristics via the soft mask branch. Our RA-performance UNets may be greatly enhanced by using the residual attention technique.

4. Results and Discussion

Some metrics are used to evaluate the performance of models:

Accuracy: Accuracy calculate how many pixels are classified correctly without any regard to the class, which is not a very good metric as the true negatives value will always be dominating by far and will always get 98%+

Dice Coefficient: It calculates the overlap between the classes of the input A and predicted label B and is calculated as follows

$$Dice = \frac{2|A\cap B|}{|A|+|B|} \qquad (3)$$

True Value Accuracy: It calculates the accuracy of segmentation for tumors and the liver and is calculated as follows

$$Accuracy = \frac{TP}{TP+FN} * 100 \qquad (4)$$

TP = True Positive; FA=False Negative;

vi) The loss function:

We learn the weights by minimizing a loss function. In this investigation, we used a loss function based on the Dice coefficient presented in the paper. The loss L is defined as follows: (5)

$$L = 1 - \frac{2\sum_{i=1}^{N} s_i g_i}{\sum_{i=1}^{N} s_i^2 + \sum_{i=1}^{N} g_i^2} \qquad (5)$$

When N is the number of voxels, s_i and g_i belong to the binary segmentation and binary ground truth voxel sets, respectively. The loss function directly quantifies the similarity between samples.

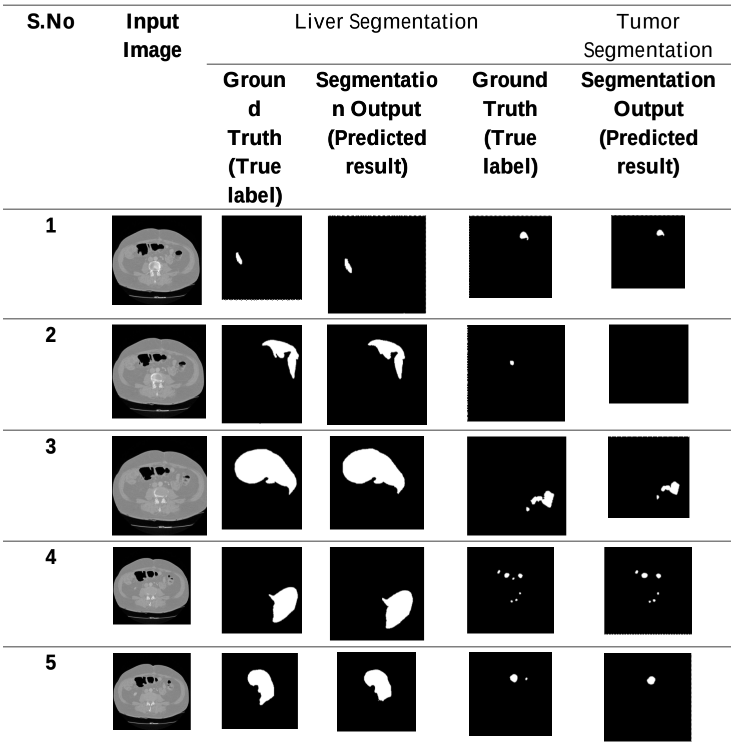

Figure.4 (a) input images, (b) ground truth images for liver segmentation, (c) Segmentation results for liver segmentation, (d) ground truth images for tumor segmentation and (e) segmentation results for tumor segmentation.

The Dice Similarity Coefficient(DSC) performance of liver segmentation with respect to the number of layers (parameters). From the training data set used in this study, the number for the best DSC performance from Wang, J et al. [24] and Ayalew, Y. A et al. [26] was 20 and 50, respectively. With a well-trained model of each network, performances were measured for the segmentation. Figure 4 shows the segmentation results from a thin slice (0.8mm) and a thick slice (5 mm). Absolute difference maps (error maps) between segmentation results of each method and ground truth are also illustrated in in figure 4 (Truth lable). For a thin slice, the segmentation and contouring results of the proposed network are the most accurate, however,

ISSN: 2582 - 4201(Online) , http://www.ijrdes.com/ , IJRDES, Vol. 6, Issue 3 , 2024 , https://doi.org/10.63328/IJRDES-V6RI3P1

other methods for comparison offer quite similar results for both liver and liver-tumor segmentation with high accuracy as well. Unlike the results from the thin slice, in the thick slice case, the proposed network has obviously excellent segmentation and contouring results of both liver and liver tumor in comparison to other methods.

Table.3 Liver training Progress

Iteration	Accuracy	Loss	Dice_Coefficient	Time (sec)
1	97.36	13.06	86.94	996
2	97.91	9.91	90	736
3	97.91	9.8	90.2	734
4	98.22	7.68	92.32	734
5	98.26	7.33	92.67	734
6	98.33	6.62	93.38	735
7	98.35	6.26	93.74	734
8	98.45	5.38	94.62	734
9	98.49	4.99	95.01	734
10	98.59	4.28	95.72	734
11	98.62	3.94	96.06	733
12	98.66	3.59	96.41	732
13	98.71	3.05	96.95	732
14	98.71	3.13	96.87	732
15	98.73	2.92	97.08	734
16	98.75	2.77	97.23	734
17	98.74	2.82	97.18	732
18	98.79	2.46	97.54	732
19	98.79	2.4	97.6	732
20	98.79	2.42	97.58	733

When verifying the results from all slices, 3D volumes of the segmentation results from the thick slice are visualized, as shown in figure 4 (**Predicted**).

Table 4. Tumor training/ testing progress

Iteration	Accuracy		Loss		Dice_Coefficient		Time (sec)
	Training	Testing/ Validation	Training	Testing/ Validation	Training	Testing/ Validation	
1	99.33	99.22	23.23	58.8	76.77	41.2	849
5	99.72	99.71	23.81	21.15	86.19	88.85	733
10	99.75	99.64	21.03	11.35	88.97	88.65	728
15	99.78	99.77	18.69	18.09	91.31	91.91	728
20	99.79	99.78	17.32	16.85	92.68	93.15	726
25	99.81	99.79	15.63	15	94.37	95	727
30	99.82	99.8	14.77	14.77	95.23	95.23	727
35	99.83	99.7	13.93	22.55	96.07	87.45	726
40	99.84	99.7	13.17	22.49	96.83	87.51	727
45	99.85	99.84	12.16	11.71	97.84	98.29	727
50	99.86	99.83	11.62	11.85	98.38	98.15	727

Volume of liver and liver-tumor segmentation obtained from the proposed network is most similar to that from the ground truth and its shows the overlaid images including liver and liver-tumor segmentation results of the Res U–Net and the ground truth, acquired from various test cases. The quantitative analysis from all test cases in Tables 3 and Table 4 also show the scores consistent with the results in figure 4. The proposed Res U-Net also attained higher scores than listed in other public databases like 3Dircadb, as listed in Table 3. The training time/epoch of Li's networks were the longest, and the evaluation was more than 7 sec.

First, we use DL as the loss function and compare the classic network mU-Net, FCN, UNet, Attention U-Net, and Attention Res U-Net. From Table 5, we can see that FCN results in the worst performance on Dice and Loss compared to the other four networks. On the other hand, compared with FCN, U-Net, Attention U-Net, and Attention Res-UNet, EAR U-Net and W-Net, the proposed RA-UNet model achieved the best performances on the four metrics (Dice, Accuracy, Loss, and Time).

Table.5 Quantitative results compared with proposed and other methods

Model	Segmentation	Dataset	Accuracy	Loss	Dice_Coefficient	Time
Proposed work	Liver	3DIRCADB	98.458	4.73	95.27	2h15m25s(8125 sec)
	Tumor		99.76 ± 0.6	7.76 ± 2.2	92.24 ± 3.41	
mU-Net[27]	Liver	3DIRCADB [27]	-	-	**96.01 ± 1.08**	-
	Tumor		-	-	68.14 ± 6.4	
FCN[27]	Liver	LiTS17[24]	-	13.83±5.83	92.46±3.52	4h31m13s
	Tumor		-	10.75±3.36	94.29±1.9	
U-Net[27]	Liver		-	11.12±3.65	94.08±2.06	7h49m13s
	Tumor		-	8.16±3.76	95.71±2.10	
Attention U-Net[27]	Liver		-	10.58±4.04	94.37±2.27	8h56m35s
	Tumor		-	7.96±2.38	95.84±1.29	
Attention Res U-Net[27]	Liver		-	9.61±2.97	94.93±1.63	9h48m56s
	Tumor		-	7.60±1.90	96.04±1.03	
EAR U-Net[27]	Liver		-	7.77±1.42	95.95±0.76	6h45m54s
	Tumor		-	6.50±1.52	96.63±0.82	
U-Net[26]	Liver	3DIRCADB [26]	99.31	-	96.12	-
	Tumor		99.54	-	74 ± 2	
W-net[14]	Liver	3DIRCADB [14]	-	8.06	95.79	1h8m50s(4130 sec)
	Tumor			14.78	66.02	

Specifically, its superiority on dice is the most significant. Therefore, RA-UNet enabled an improvement in the accuracy and stability of the segmentation. Besides, in terms of training time, RA-UNet is far less than when compare to the other deep learning networks. However, in terms of test time, the RA-UNet is acceptable when compare to the other networks.

5. Conclusion

This article concludes with the presentation of a more robust deep learning network for segmentation, which might provide more accurate results than previous networks in liver and tumor areas, even when the border is unclear, and the target item is tiny. By incorporating the residual path and an object-dependent up sampling design, the proposed network avoids duplication of low-resolution information, estimates higher

ISSN: 2582 - 4201(Online) , http://www.ijrdes.com/ , IJRDES, Vol. 6, Issue 3 , 2024 , https://doi.org/10.63328/IJRDES-V6RI3P1

level feature maps that more accurately represent the high-resolution edge information of larger object inputs, and learns to extract even higher level global features for small object inputs. The suggested approach does not need any preprocessing. Hence, it applies to various organs and pictures with low contrast. It might also be used for medical pictures from other imaging modalities, such as MRI, PET, or ultrasound.

References

[1] Bilic, P., Christ, P. F., Vorontsov, E., Chlebus, G., Chen, H., Dou, Q., ... & Menze, B. H. (2019). The liver tumor segmentation benchmark (lits). *arXiv preprint arXiv:1901.04056*.

[2] Fournier, L., de Geus-Oei, L. F., Regge, D., Oprea-Lager, D. E., D'Anastasi, M., Bidaut, L., ... & Caramella, C. (2021). Twenty years on: RECIST as a biomarker of response in solid tumours an EORTC imaging group–ESOI joint paper. *Frontiers in Oncology*, *11*.

[3] Chi, Y., Wang, D., Wang, J., Yu, W., & Yang, J. (2019). Long non-coding RNA in the pathogenesis of cancers. *Cells*, *8*(9), 1015.

[4] Alirr, O. I. (2020). Deep learning and level set approach for liver and tumor segmentation from CT scans. *Journal of Applied Clinical Medical Physics*, *21*(10), 200-209.

[5] Rela, M., Suryakari, N. R., & Reddy, P. R. (2020). Liver tumor segmentation and classification: a systematic review. *2020 IEEE-HYDCON*, 1-6.

[6] Gotra, A., Sivakumaran, L., Chartrand, G., Vu, K. N., Vandenbroucke-Menu, F., Kauffmann, C., ... & Tang, A. (2017). Liver segmentation: indications, techniques and future directions. *Insights into imaging*, *8*(4), 377-392.

[7] Calisto, M. B., & Lai-Yuen, S. K. (2020). AdaEn-Net: An ensemble of adaptive 2D–3D Fully Convolutional Networks for medical image segmentation. *Neural Networks*, *126*, 76-94.

[8] Li, C., Tan, Y., Chen, W., Luo, X., He, Y., Gao, Y., & Li, F. (2020). ANU-Net: Attention-based Nested U-Net to exploit full resolution features for medical image segmentation. *Computers & Graphics*, *90*, 11-20.

[9] Li, X., Chen, H., Qi, X., Dou, Q., Fu, C. W., & Heng, P. A. (2018). H-DenseUNet: hybrid densely connected UNet for liver and tumor segmentation from CT volumes. *IEEE transactions on medical imaging*, *37*(12), 2663-2674.

[10] Gan, H. S., Ramlee, M. H., Wahab, A. A., Lee, Y. S., & Shimizu, A. (2021). From classical to deep learning: review on cartilage and bone segmentation techniques in knee osteoarthritis research. *Artificial Intelligence Review*, *54*(4), 2445-2494.

[11] Bui, V., Shanbhag, S. M., Levine, O., Jacobs, M., Bandettini, W. P., Chang, L. C., ... & Hsu, L. Y. (2020). Simultaneous multi-structure segmentation of the heart and peripheral tissues in contrast enhanced cardiac computed tomography angiography. *IEEE Access*, *8*, 16187-16202.

[12] Rundo, L., Stefano, A., Militello, C., Russo, G., Sabini, M. G., D'Arrigo, C., ... & Gilardi, M. C. (2017). A fully automatic approach for multimodal PET and MR image segmentation in Gamma Knife treatment planning. *Computer Methods and Programs in Biomedicine*, *144*, 77-96.

[13] Nayantara, P. V., Kamath, S., Manjunath, K. N., & Rajagopal, K. V. (2020). Computer-aided diagnosis of liver lesions using CT images: a systematic review. *Computers in Biology and Medicine*, *127*, 104035.

[14] Li, J., Ou, X., Shen, N., Sun, J., Ding, J., Zhang, J., ... & Wang, Z. (2021). Study on strategy of CT image sequence segmentation for liver and tumor based on U-Net and Bi-ConvLSTM. *Expert Systems with Applications*, *180*, 115008

[15] Yamashita, R., Nishio, M., Do, R. K. G., & Togashi, K. (2018). Convolutional neural networks: an overview and application in radiology. *Insights into imaging*, *9*(4), 611-629.

[16] Alom, M. Z., Yakopcic, C., Hasan, M., Taha, T. M., & Asari, V. K. (2019). Recurrent residual U-Net for medical image segmentation. *Journal of Medical Imaging*, *6*(1), 014006.

[17] Kamnitsas, K., Ledig, C., Newcombe, V. F., Simpson, J. P., Kane, A. D., Menon, D. K., ... & Glocker, B. (2017). Efficient multi-scale 3D CNN with fully connected CRF for accurate brain lesion segmentation. *Medical image analysis*, *36*, 61-78.

[18] Yang, Z., Zhao, Y. Q., Liao, M., Di, S. H., & Zeng, Y. Z. (2021). Semi-automatic liver tumor segmentation with adaptive region growing and graph cuts. *Biomedical Signal Processing and Control*, *68*, 102670.

[19] Allioui, H., Sadgal, M., & El Fazziki, A. (2020). An improved image segmentation system: a cooperative multi-agent strategy for 2D/3D medical images. *Journal of Communications Software and Systems*, *16*(2), 143-155.

[20] Gotra, A., Sivakumaran, L., Chartrand, G., Vu, K. N., Vandenbroucke-Menu, F., Kauffmann, C., ... & Tang, A. (2017). Liver segmentation: indications, techniques and future directions. *Insights into imaging*, *8*(4), 377-392.

[21] Anter, A. M., & Hassenian, A. E. (2019). CT liver tumor segmentation hybrid approach using neutrosophic sets, fast fuzzy c-means and adaptive watershed algorithm. *Artificial intelligence in medicine*, *97*, 105-117.

[22] Christ, P. F., Ettlinger, F., Grün, F., Elshaera, M. E. A., Lipkova, J., Schlecht, S., ... & Menze, B. (2017). Automatic liver and tumor segmentation of CT and MRI volumes using cascaded fully convolutional neural networks. *arXiv preprint arXiv:1702.05970*.

[23] Baâzaoui, A., Barhoumi, W., Ahmed, A., & Zagrouba, E. (2017). Semi-automated segmentation of single and multiple tumors in liver CT images using entropy-based fuzzy region growing. *IRBM*, *38*(2), 98-108.

[24] Wang, J., Zhang, X., Lv, P., Zhou, L., & Wang, H. (2021). EAR-U-Net: EfficientNet and attention-based residual U-Net for automatic liver segmentation in CT. *arXiv preprint arXiv:2110.01014*.

[25] Ibtehaz, N., & Rahman, M. S. (2020). MultiResUNet: Rethinking the U-Net architecture for multimodal biomedical image segmentation. *Neural networks*, *121*, 74-87.

[26]. Ayalew, Y. A., Fante, K. A., & Mohammed, M. A. (2021). Modified U-Net for liver cancer segmentation from computed tomography images with a new class balancing method. *BMC Biomedical Engineering*, *3*(1), 1-13.

[27] Seo, H., Huang, C., Bassenne, M., Xiao, R., & Xing, L. (2019). Modified U-Net (mU-Net) with incorporation of object-dependent high level features for improved liver and liver-tumor segmentation in CT images. *IEEE transactions on medical imaging*, *39*(5), 1316-1325.

ISSN: 2582 - 4201(Online) , http://www.ijrdes.com/ , IJRDES, Vol. 6, Issue 3 , 2024 , https://doi.org/10.63328/IJRDES-V6RI3P1

Author Profile

P.Gangadhara Reddy is currently working as Associate Professor in department of ECE,Aditya College of Engineering,Madanapalle. He Completed Ph.D in the area of Medical Image Processing Using Machine Learning Algorithms from S.V.U College of Engineering, S.V.University, Tirupati, Andhra Pradesh, India. He completed his M.Tech degree in Electronic Instrumentation and Communication Systems from S.V.U. College of Engineering, S.V.University, Tirupati and B.Tech in ECE from Rajiv Gandhi College of Engineering &Technology, Nandyal. He has published 18 technical papers in different reputed International and National journals and International conferences. His areas of research interest include Medical Image Processing,Deep Learning and Machine Learning. He is a Life Member of ISTE and ISRD.

Dr. T. Ramashri is currently Professor and Head, Department of Electronics and Communication Engineering, S.V. University College of Engineering, S.V. University, Tirupati, Andhra Pradesh, India. She has 30 years of experience in teaching and research at the Undergraduate, Postgraduate and Ph.D levels. Her main areas of interest are Signal Processing Techniques, Digital Image Processing and VLSI Design. As of date, she has guided 15 Ph.D students and currently six scholars are pursuing. She has published over 120 papers in reputed indexed international journals and proceedings of national and international conferences. She is a Senior Member of IEEE, Fellow of IETE, Life Member of ISTE and acting as Member in Editorial Board of reputed indexed journals.